

Thermal tar cracking enhanced by cold plasma - a study of naphthalene as tar surrogate

Yamid Gomez-Rueda^a, Ilman Nuran Zaini^c, Weihong Yang^c, Lieve Helsen^{a,b}

^a*Department of Mechanical Engineering, Celestijnenlaan 300, Leuven 3001, Belgium*

^b*Energyville, Thor Park, Waterschei, Belgium*

^c*Department of Materials Science and Engineering, KTH Royal Institute of Technology, 100 44 Stockholm, Sweden*

Abstract

Gasification has been proposed as a good solution for recovering energy from waste and biomass in the form of syngas. However, the presence of tar limits syngas applications. Tar model molecules have been removed by cold plasmas up to 400°C, but to avoid syngas cooling tar removal above 600°C is required. To investigate tar removal by cold plasma at higher temperatures, two sets of experiments were done, one to identify tar composition from MSW gasification, and a second one to crack in a nanosecond-pulsed corona plasma at high temperatures the most refractory tar compound found, naphthalene. In this paper, we report the first results of cold plasma for tar cracking at temperatures up to 1100°C, revealing that this tandem can remove naphthalene completely at 800°C, compared to the 1000°C needed in case of thermal cracking alone. The synergy between plasma and thermal cracking is driven by higher energy densities when temperatures increase. However, this synergy stops when thermal cracking reactions predominate.

Keywords: Gasification, Municipal Solid Waste, Cold Plasma, Tar Removal, Naphthalene

1. Introduction

Tar is a set of substances produced as a byproduct during the gasification of carbon-rich feedstock, such as Municipal Solid Waste (MSW), and its removal from syngas has been identified as one of the major challenges in gasification [1]. Although tar is a major factor in environmental pollution from gasification due to its toxic nature [2, 3], the main operational problem associated with tar is its capacity of condensing at high temperatures, which eventually causes clogging of piping and equipment, increasing maintenance times to inadmissible levels [4]. These maintenance times are critical for appliances such as gas turbines and engines, where the small injectors are prone to be blocked. Tar can also cause the deactivation of catalysts by coking, which hampers tar-polluted syngas to be used in fuel cells [5, 6, 7, 8], in methanation [9] and in Fischer-Tropsch synthesis.

Although there are some methods that take advantage of the ease of tar condensation to remove them, it is preferred to crack them to produce more syngas to avoid cooling (which is needed for condensation) in order to recover the sensible heat contained in the syngas. Cooling should be avoided if the downstream valorization processes are also carried out at high temperatures, such as in the case of methanation (operating at 500-700°C) [10] or Solid Oxide Fuel Cells (SOFCs operating between 750-950°C) [11]. Even if the subsequent valorization is carried out at lower temperatures, such as in Fischer-Tropsch or Proton-Exchange Membranes (PEM) fuel cells, cracking tar at the high temperature of the gasifier outlet is still beneficial since tar cracking reactions are endothermic.

So far, thermal and catalytic cracking have shown to be able to remove

26 tar to a high extent but the use of excessive temperatures in the former case
27 (usually above 1000-1250°C) [12, 13, 14, 15], and the short lifetime due to
28 coking [16], sulfur [17] or evaporation for the latter case does not allow them
29 to be used extensively in the industry [18]. Some alternative approaches,
30 like the addition of activated carbons and biochar, can be effectively used in
31 certain lab conditions for tar removal [19, 20, 21], but not in real large-scale
32 gasifiers due to carbon consumption by steam and oxygen reactions.

33 Therefore, plasma has arisen as a new solution for tar cracking. Thermal
34 plasmas, which exhibit high temperatures (above 4000K) have been exten-
35 sively used for MSW gasification in primary units [22, 23, 24, 25, 26] but also
36 in secondary units for tar cracking. Materazzi et al. [27] have demonstrated
37 that a thermal plasma secondary unit can convert tar into CO instead of soot,
38 by using a plasma torch operating in a temperature range of 5500–10,000°C.
39 It has also been reported that the high temperatures alone are not able to
40 remove some tar components such as naphthalene and benzene; naphthalene
41 and benzene removal needs the combined effect of plasma excited species and
42 high-temperature [28].

43 Although tar has been successfully removed with thermal-plasmas, the
44 energy demand of such plasmas is large, making this technology feasible only
45 when electricity is extremely cheap, or when difficult-to-treat inputs (such
46 as dangerous waste) is used as feedstock [29]. For instance, Marias et al.
47 [30] determined that a plasma torch of 240kW needed to produce a syngas
48 with a power of 1616kW , which is an enormous amount of high quality
49 energy (electricity) needed as input. The extreme gas heating up in thermal
50 plasma cracking might require as well extra cooling down of the producer

51 gas for downstream applications. This has opened a window for using delete
52 intensive plasmas, such as warm and cold plasmas which are less heated.

53 The main difference between cold plasmas and thermal plasmas is the
54 equilibrium temperature of the plasma species. While in thermal plasmas all
55 species are in thermal equilibrium, in cold plasmas the electron temperature
56 is higher than the temperature of the other species. This means that the gas
57 is not heated-up by the plasma, but it is still exposed to high-energy electrons,
58 generating excited molecules, ions, and UV radiation. In the case of warm
59 plasmas, there is still a non-equilibrium temperature among all the species,
60 but some degree of heating is achieved. In tar cracking, Dielectric Barrier
61 Discharge (DBD) and corona plasmas are the main cold plasma technologies
62 used, and gliding arc discharge (GAD) is the main warm-plasma technology
63 used.

64 Although GADs have shown to be effective for tar model compounds
65 removal alone [10, 31, 32, 33, 34] or in combination with catalysts [35, 36, 37],
66 the need of syngas cooling after such units is still there. However, by using
67 cold plasmas (DBD and corona) there is a negligible gas heating, discarding
68 the need of any downstream syngas cooling.

69 The main difference between the two cold plasma technologies mentioned
70 lies in the type of voltage source used: while DBD uses AC, corona uses
71 DC. This has many implications, one is that while DBD plasmas need a
72 dielectric material around one or two of the electrodes, corona plasmas do
73 not need any dielectric. Unfortunately, corona plasmas can easily transit
74 towards a spark and are more difficult to control. The other main difference
75 is that DBD plasmas are naturally pulsed due to the AC energy source, while

76 corona plasmas need an extra unit in order to generate a pulsed discharge.

77 DBD plasma units have been the most explored cold plasma technologies
78 in lab-scale experiments for tar removal, either alone or in combination with
79 catalysts. Although some authors have studied the DBD plasma alone, like
80 Saleem et al. [38], for the removal of benzene, or Wu et al. [39] in the removal
81 of naphthalene, most of the studies have been performed using plasma in
82 combination with catalysts. For instance, Liu et al. showed that an M1Al3
83 catalyst in a plasma reactor can achieve toluene conversions higher than
84 95% with benzene and ethylbenzene as main reaction products [40]. Similar
85 works using a plasma combined with in-situ Ni/Al₂O₃ and Ni/ZSM show
86 an enhanced conversion of toluene with a simultaneous soot reduction [41,
87 42] when compared to plasma cracking alone. Naphthalene has been also
88 successfully removed in similar plasma-catalytic systems [36, 43, 44].

89 Corona plasmas have been used in few cases for the conversion of naph-
90 thalene and hydrocarbons. Nair et al. were able to remove naphthalene at
91 400°C at residence times of 3 min [45] and Bityurin et al. demonstrated that
92 carbon monoxide reduced naphthalene cracking activity when compared to
93 a pure nitrogen atmosphere [46]. The reduced use of corona plasma with
94 respect to DBD is due to the difficult generation of pulses, which requires
95 the use of high voltage resistors to limit the current, requiring careful design
96 to avoid sparks in the HV system. However, the lack of any dielectric ma-
97 terial in corona plasmas makes them interesting for using them at the high
98 temperatures found at the exit of gasifiers.

99 However, removing tar at low temperatures has very little advantage in
100 comparison to wet scrubbing using organic solvents (except that liquid waste

101 streams are avoided), because it forces the gas exiting the gasifier to be
102 cooled-down for cleaning, requiring a reheating after the cleaning process for
103 ultimate valorization. So far the highest reported operating temperature on
104 which a cold-plasma cracking unit has operated is 400°C for corona plasma
105 [45]and 400°C for DBD plasmas [47].

106 There is thus a need for operating cold plasma systems at higher tem-
107 peratures. In this paper, two sets of experiments are described in order to
108 evaluate a nanosecond pulsed corona plasma for tar removal at high temper-
109 atures. The first set of experiments focused on the characterization of tar
110 resulting from gasification of MSW from steam and air atmospheres. In this
111 analysis it is used the standard definition of tar given by the EU/IEA/US-
112 DOE panel, which considers as tar as all the organic compounds of a higher
113 molecular weight than benzene [48], and it is also used the tar classification
114 made by the Energy Research Center of the Netherlands (ECN) [49] showed
115 in table 1 in order to understand tar evolution. The second set of experi-
116 ments focused on cracking the most stable tar molecule identified in the first
117 part in a nanosecond pulsed corona plasma under a nitrogen atmosphere.

118 **2. Experimental**

119 The feedstock for the first set of experiments was a MSW sample with the
120 fraction and composition given in table 2. The gasification reactor consists
121 of a stainless-steel 316 cylinder with two temperature zones, one cold and
122 one hot. The MSW sample was kept in the cold zone, around 20°C, while
123 the hot zone of the reactor reached the desired temperature. The reactor was
124 kept under a flow of N₂ while heating-up. The sample was then moved to the

Table 1: Tar compound classification according to ECN [49]. Acronyms: GC = Gas Chromatography, PAH = Polycyclic Aromatic Hydrocarbons.

| Nomenclature | Description | Properties | Representative compounds |
|--------------|---------------------------------------|---|--|
| Class 1 | GC-undetectable | Very heavy tar; undetectable by GC | Biomass fragments; heaviest tar |
| Class 2 | Heterocyclic aromatics | Tar containing hetero atoms; highly water soluble | Pyridine, phenol, quinoline, isoquinoline, cresols |
| Class 3 | Light aromatic (1 ring) | Light hydrocarbons; do not pose condensation or solubility problems | Toluene, ethylbenzene, xylenes, styrene |
| Class 4 | Light PAH compounds (2-3 rings) | Condense at intermediate temperatures at high concentrations | Indene, naphthalene, methylnaphthalene, phenanthrene, anthracene |
| Class 5 | Heavy PAH compounds (≥ 4 rings) | Condense at high temperatures even at low concentrations | Fluoranthene, pyrene, crysene, perylene, coronene |

125 hot-zone and kept under a flow of air for 60 min, with an Equivalence Ratio
 126 (ER) of 0.3 for air gasification experiments with and air flow of 95ml/min
 127 and a steam-to-waste ratio of 0.5 for steam gasification experiments.

128 The sample weight during all the experiments was 5 g. The steam was
 129 injected by a boiler unit connected by a three-way valve to the main reactor.
 130 The steam was injected once the boiler steady-state was reached and checked
 131 by measuring the steam condensation in a parallel process. The tar gener-
 132 ated was sampled by the Solid-phase Adsorption - Solid-phase Extraction
 133 (SPA/SPE) method as stated by Brage et al. [50] and the gas released was
 134 collected in a Tedlar-gas bag for being analyzed off-line by a micro-GC. A
 135 scheme of the experimental setup is presented in figure 1.

136 For the second part of the experiments, only one tar model molecule was
 137 chosen based on the results of the first series of experiments. The equipment

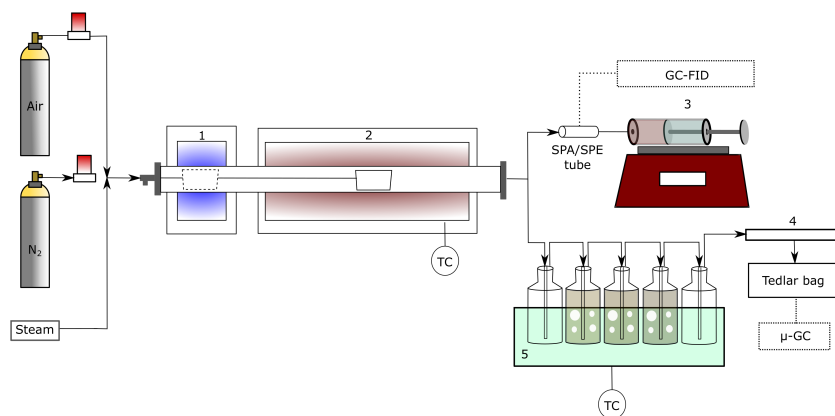


Figure 1: Gasification reactor. Parts: 1. Reactor cold zone. 2. Reactor hot-zone. 3. SPA/SPE sampling setup 4. Glass wool filter. 5. Series of bottles for tar condensation, three of them contain acetone while the other two are empty.

138 used in this part consists of a High-Voltage Direct-current (HV DC) power
 139 unit with 24kV voltage and 5mA current connected to an RC-circuit which
 140 allows producing short DC pulses by using a spark-gap switch filled-up with
 141 nitrogen. The pulses are then transmitted through a coaxial cable to a reactor
 142 that is placed inside a three-zone oven. The reactor consist of a FeCrAl pipe
 143 of 1.27m length and 64mm diameter.

144 Upstream of the reactor, a saturator filled up with the objective molecule
 145 is kept at a temperature of $70\pm 1^\circ\text{C}$. A carrier nitrogen stream of 2NL/min
 146 (normal liter per minute) passes trough the saturator which is mixed-up with
 147 a second nitrogen stream of 2NL/min before entering the plasma reactor.
 148 The residence time in the plasma reactor is set to 30s in order to obtain
 149 an appreciable energy density (see equation 2). Between each temperature
 150 test, the reactor was flushed with air for 20 min to remove the soot produced
 151 and then again purged with nitrogen for 10 min. The tar concentration

Table 2: Waste fractions, proximate and ultimate analysis of the MSW samples used in gasification tests

| Waste fraction | Fraction (wt%, dry basis) |
|-------------------|---------------------------|
| Wood | 1 |
| Paper | 4 |
| Textile | 9 |
| 2D plastics | 39 |
| 3D plastics | 5 |
| Other combustible | 11 |
| Fines | 31 |

| Proximate composition (wt.%, db) | |
|----------------------------------|------|
| Volatile matter | 55.3 |
| Fixed carbon | 1.8 |
| Ash | 46.5 |
| Ultimate composition (wt.%, db) | |
| C | 40.5 |
| H | 6.1 |
| N | 1.1 |
| O | 4.3 |
| S | 0.2 |
| Cl | 1.2 |
| LHV (MJ/kg, db) | 22.9 |

152 was evaluated by the SPA/SPE method, by sampling 100ml of gas at the
 153 bottom of the reactor after each test, with a blank test taken before each
 154 test. Between three to five samples were taken for each experiment after
 155 25-30 minutes of achieving steady-state. All gas lines, including the SPA
 156 sampling lines, are heated at a temperature between 105-110°C. A scheme
 157 of the experimental setup is shown in figure 2. The plasma discharge was
 158 followed by a Handyscope HS4 DIFF from the company TiePie.

159 *2.1. Performance indicators*

160 In order to evaluate the thermal-plasma tar removal process, multiple
 161 indicators need to be calculated. One of these performance indicators is the
 162 energy per pulse delivered by the plasma, which is determined by equation
 163 1 from the voltage-current curves presented in figure 3.

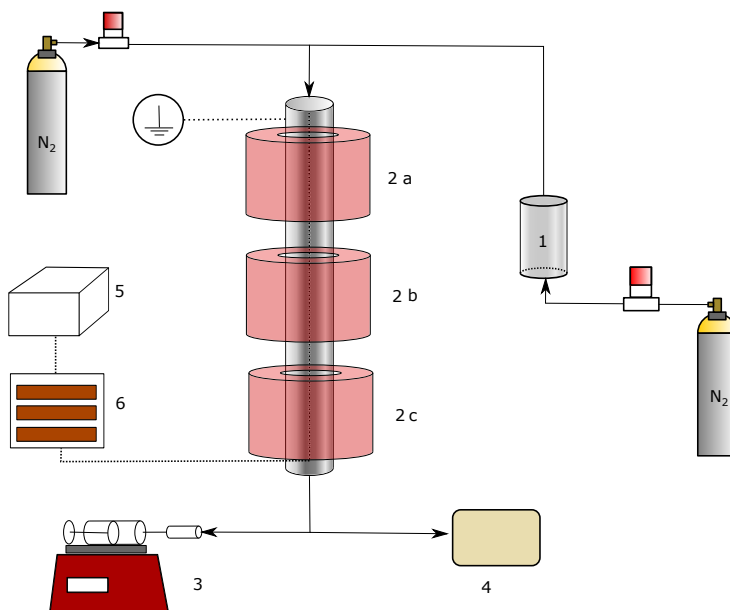


Figure 2: HV nanosecond pulsed corona plasma reactor setup. Parts: 1. Tar model molecule saturator. 2a,b,c. Three-zone convection oven. 3. SPA/SPE sampling 4. Exhaust. 5. HV DC power supply. 6. Pulse generator

$$E_p = \int_0^{t=500ns} U(t)I(t)dt \quad (1)$$

164 where E_p is the energy per pulse in mJ per pulse, $U(t)$ represents the
 165 instantaneous voltage in V and $I(t)$ represents the instantaneous current in
 166 A. Another parameter for evaluating the tar removal efficiency is the specific
 167 energy input (SEI) or energy density, which is calculated using equation 2
 168 where E_p is the energy per pulse determined by equation 1 in mJ per pulse,
 169 ν is the frequency of the pulses in pulses per second, and \dot{Q} is the volumetric
 170 flow of nitrogen carrying the tar model molecule in normal liters per minute.
 171 The SEI units are J/L.

$$SEI = \frac{E_p * \nu * 60}{\dot{Q} * 1000} \quad (2)$$

172 The conversion of the tar model molecule in the plasma tar cracking
 173 experiments is determined by using equation 3 where C_o represents the initial
 174 concentration of the model compound, which was taken when the reactor was
 175 heated at 100°C , while C_f represents the final concentration.

$$\eta(\%) = \frac{C_o - C_f}{C_o} * 100 \quad (3)$$

176 The energy efficiency or energy removal efficiency, (EE) of the plasma pro-
 177 cess is evaluated by equation 4, where $[C]_{on}$ and $[C]_{off}$ are the concentrations
 178 leaving the reactor when the corona plasma is on and off respectively,

$$EE = \frac{[C]_{off} - [C]_{on}}{SEI} \quad (4)$$

179 A final significant parameter is the energy efficiency parameter β (also
 180 known as characteristic energy or energy cost) of the model molecule destruc-
 181 tion process. It is calculated from plotting the exponential decrease of the
 182 model molecule concentration versus SEI, as in equation 5 [51, 52] where β
 183 and the SEI are given in J/L.

$$\frac{[C]_{on}}{[C]_{off}} = \exp\left(\frac{SEI}{-\beta}\right) \quad (5)$$

184 **3. Results and discussion**

185 *3.1. Identification of tar representative molecules*

186 The first part of the experiments consists of gasification experiments us-
 187 ing air and steam for the light MSW fraction in the setup described in figure

Table 3: Gasification experimental matrix

| Gas agent | Temperature | Sample ID |
|-----------|-------------|------------|
| Air | 800°C | Air-800 |
| | 1100°C | Air-1100 |
| Steam | 800°C | Steam-800 |
| | 1100°C | Steam-1100 |

188 1. The experimental matrix is shown in table 3. The objective of this exper-
 189 imental program is to evaluate the tar speciation at different temperatures
 190 and using different gas agents, but also to determine which compounds are
 191 more difficult to remove by thermal cracking.

192 The tar composition of these experiments is presented in tables 4 and 5
 193 which are analyzed with respect to total tar, phenolic compounds concentra-
 194 tion, and aromatic compounds distribution. At first sight, the temperature
 195 increase causes a reduction in the total tar yield. For air gasification, the
 196 effect is evident, but not for steam. Although total tar yield is almost the
 197 same in both experiments with steam, at 1100°C the presence of benzene is
 198 much higher. Considering that benzene is quantified but it does not enter
 199 into the definition of tar, then the tar yield reduction is more clear.

200 Regarding phenolic compounds, presented in table 5, they are present in
 201 very low quantities at 800°C, and totally disappear at 1100°C. Due to these
 202 two reasons, we can leave out of consideration these compounds in the second
 203 set of experiments.

204 The aromatic compounds represent between 97 and 100% of the total
 205 tar yield in all experiments. At 800°C, besides benzene the two most abun-

206 dant compounds are toluene and naphthalene for air and o-xylene, naphtha-
207 lene and indene for steam. At high temperatures, the most representative
208 molecules are naphthalene and acenaphthylene for air and naphthalene and
209 benzene for steam. In all cases naphthalene appears as one of the most
210 representative tar molecules, especially at high temperatures where it is by
211 far the most abundant compound in both air and steam gasification. This
212 makes naphthalene the most interesting molecule to be chosen for the sec-
213 ond part of the experiments, which coincides with previous studies that have
214 chosen naphthalene as tar model molecule in biomass and coal gasification
215 [35, 53, 54].

216 Other molecules that can be problematic are the polyaromatic hydro-
217 carbons (PAHs) such as acenaphthylene, phenanthrene, fluoranthene, and
218 pyrene. During the experiments, PAHs compounds concentration increases
219 with temperature, and although their concentration is still very low with
220 respect to other compounds, PAHs have a higher impact in tar dew point.
221 This means that the tar remaining after tar cracking at high temperatures is
222 more stable and more prone to condensation than the tar remaining at low
223 temperatures.

224 The tar composition presented here differs from the tar composition pre-
225 sented in other publications using other types of feedstock such lignite [55],
226 bituminous coal [56], woody biomass [57], sewage sludge [58, 59]. Even com-
227 pared with other MSW, [60, 61] tar composition is very different, mainly due
228 to the MSW composition. However, in most of the studies, naphthalene is
229 among the most abundant tar molecules [57, 58, 59, 60, 62, 63, 64] and the
230 most difficult aromatic compound to be destroyed by thermal cracking, after

Table 4: Aromatic compounds found during steam and air gasification of MSW. Concentrations are given in $\mu\text{g}/100\text{ml}$. ND = Not detected (below the limit of detection)

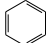
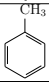
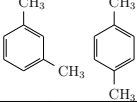
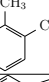
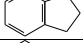
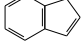
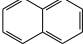
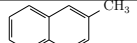
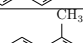
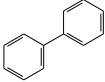
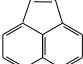
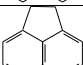
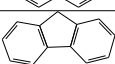
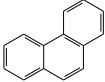
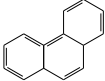
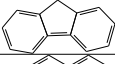
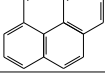
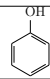
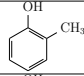
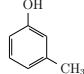
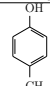
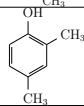
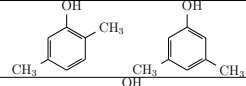
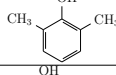
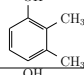
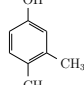
| | Temperature | 800°C | 1100°C | 800 °C | 1100°C |
|---|-----------------------|-------|--------|--------|--------|
| Structure | Gasification agent | Air | Air | Steam | Steam |
|  | Benzene | 10.45 | 2.38 | N.D | 5.24 |
|  | Toluene | 18.77 | 1.42 | 0.73 | 1.56 |
|  | m/p-Xylene | 2.83 | 0.37 | 1.33 | N.D |
|  | o-Xylene | 2.18 | 2.9 | 6.3 | 2.16 |
|  | Indan | 0.42 | N.D | 0.32 | 0.04 |
|  | Indene | 3.59 | 1.63 | 2.42 | 1.1 |
|  | Naphthalene | 6.59 | 13.59 | 4.02 | 5.24 |
|  | 2-Methylnaphthalene | 1.91 | 0.24 | 1.37 | 0.13 |
|  | 1-Methylnaphthalene | 1.25 | 0.16 | 0.86 | 0.11 |
|  | Biphenyl | 0.69 | 0.81 | 0.53 | 0.37 |
|  | Acenaphthylene | 1.12 | 3.93 | 0.65 | 1.33 |
|  | Acenaphthene | 0.2 | 0.1 | 0.2 | 0.03 |
|  | Fluorene | 0.56 | 0.53 | 0.41 | 0.22 |
|  | Phenanthrene | 0.73 | 2.53 | 0.49 | 0.87 |
|  | Anthracene | 0.23 | 0.54 | 0.16 | 0.2 |
|  | Fluoranthene | 0.07 | 1.19 | 0.05 | 0.46 |
|  | Pyrene | 0.16 | 1.41 | 0.1 | 0.38 |
| Total tar | (Phenolic + Aromatic) | 51.92 | 33.81 | 20.33 | 19.99 |

Table 5: Phenolic compounds found during steam and air gasification of MSW. Concentrations are given in $\mu\text{g}/100\text{ml}$. ND = Not detected (below the limit of detection).

| | Temperature | 800°C | 1100°C | 800 °C | 1100°C |
|---|--------------------|-------|--------|--------|--------|
| Structure | Gasification agent | Air | Air | Steam | Steam |
|  | Phenol | 0.13 | 0.08 | 0.13 | 0.55 |
|  | o-Cresol | 0.01 | N.D | 0.1 | N.D |
|  | m-Cresol | 0.01 | N.D | N.D | N.D |
|  | p-Cresol | 0 | N.D | 0.09 | N.D |
|  | 2,4-Xylenol | N.D | N.D | N.D | N.D |
|  | 2,5/3,5-Xylenol | N.D | N.D | N.D | N.D |
|  | 2,6-Xylenol | 0.01 | N.D | 0.07 | N.D |
|  | 2,3-Xylenol | N.D | N.D | N.D | N.D |
|  | 3,4-Xylenol | 0.01 | N.D | N.D | N.D |

231 benzene [65, 27].

232 3.2. Plasma cracking experiments

233 3.2.1. Characterisation of the plasma discharges

234 The plasma pulses were kept between 70-72 pps (pulses per second)
 235 throughout the whole temperature range. The voltage and current pulses
 236 shapes were very similar during all discharges. The voltage pulse had an
 237 oscillating behavior, with a peak voltage of 20kV, with a duration of 30ns

238 and two more peaks of a similar duration but characterized by lower voltage.
 239 These characteristics can be seen in the voltage-current curves at different
 240 temperatures presented in figure 3.

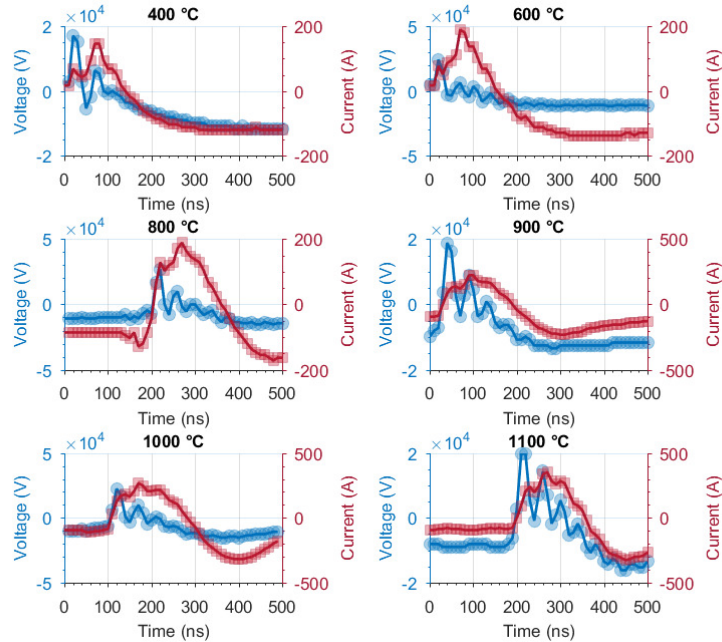


Figure 3: Plasma discharges over nitrogen polluted with naphthalene at different temperatures. Blue represents Voltage and Red represents Current.

241 The energy per pulse at each temperature can be calculated from the
 242 voltage-current curves by using the equation 1, in a similar way as used
 243 in previous publications [31]. By using equation 2 the SIE variation with
 244 temperature can be calculated. The calculated SEI at each temperature is
 245 shown in figure 4.

246 There is a direct proportionality between SEI and temperature, however,
 247 it is not clear whether it follows a linear or exponential trend. The evolution

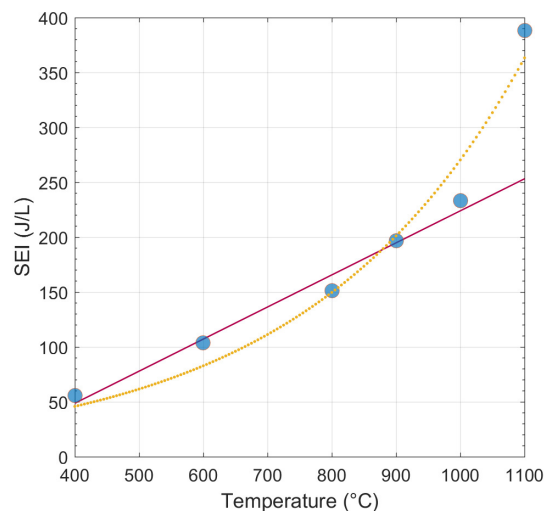


Figure 4: SEI variation with temperature. Points represent experiments, the yellow dotted line is an exponential regression, the red solid line is a linear regression (excluding the last point).

248 before 1000°C suggest a linear dependency (with a $R^2=0.98$) which was
 249 also found by other authors [45, 46, 66] but the high SEI value at 1100°C
 250 indicates that an exponential trend (with an $R^2=0.95$) can also describe this
 251 evolution.

252 3.2.2. Naphthalene cracking experiments

253 The plasma setup, described in the Experimental section and shown in
 254 figure 2 is used to crack naphthalene at temperatures between 400°C and
 255 1100°C. The initial concentration of naphthalene was set at 1.6 g/Nm³ (Nm³
 256 refers to Normal cubic meters) or around 300 ppm.

257 These experiments confirm that naphthalene requires temperatures higher
 258 than 1000°C in order to be fully cracked by thermal cracking. This tempera-
 259 ture is slightly lower than the temperatures already reported for naphthalene

260 cracking [15, 65] due to the longer residence time used in this study together
261 with a possible catalytic effect of the FeCrAl oxide present in the inner walls
262 of the reactor. The use of plasma reduces this temperature to 800°C which
263 means that a clean gas could be obtained by introducing a plasma at a lower
264 temperature. The results of naphthalene cracking are shown in figure 6a,
265 showing a clearer trend than previously published results [67].

266 An additional observation in figure 6a, which can be confirmed by ob-
267 serving figure 6b, is that there is a point (around 900 °C) where thermal
268 cracking reactions are more extensive than plasma cracking reactions. In fig-
269 ure 6b where energy efficiency(EE) is plotted against temperature, it can be
270 observed that below 800°C the EE increases with temperature, but beyond
271 this point, EE drops sharply. This behavior can also be seen in the variation
272 of energy cost (β), which varies inversely with EE, showing its lowest value
273 at 800°C. (see figure 5).

274 An explanation can be found in the fact that up to 800°C the amount
275 of naphthalene present in the gas is high enough to allow all (or most of)
276 the reactive plasma species to be consumed by reacting with naphthalene
277 (reaction R2, see next section). Above this point, the naphthalene concen-
278 tration is reduced mainly by thermal cracking, making the excited species to
279 be consumed by collisions with bulk gas molecules, reactor walls and other
280 excited molecules (reaction R3 and R4, see next section), which consequently
281 reduces the energy efficiency. The EE drop is enhanced by the fact that the
282 SEI increases with temperature.

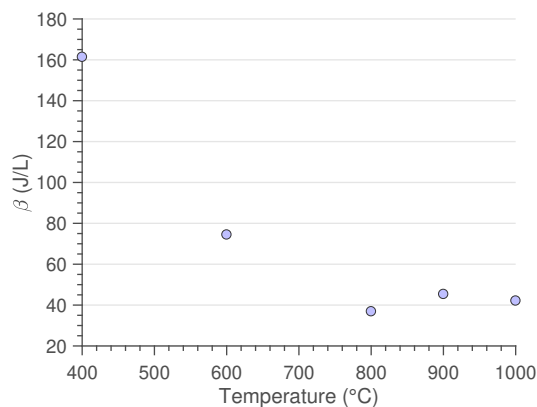


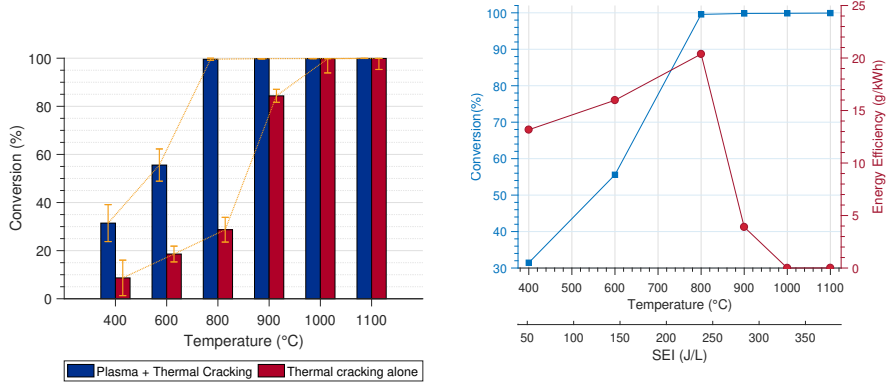
Figure 5: Specific energy cost β variation with temperature

283 *3.2.3. Kinetics of plasma naphthalene cracking*

284 In order to evaluate the efficiency of the plasma removal process, the 0D-
 285 global kinetics approach for pollutant removal proposed by Yan et al. [68] is
 286 adapted to the nanosecond pulsed naphthalene removal process. According
 287 to this approach the naphthalene plasma removal process can be described by
 288 the reactions R1 to R4. In these reactions N_2^* represents reactive radicals, and
 289 N_2 represents the bulk gas, which consists mainly of ground-state nitrogen
 290 molecules ($N_2(X^1\Sigma_g^+)$)

291 The process starts with reaction R1 by the production of reactive radicals.
 292 The following three reactions represent 3 possible ways in which the reactive
 293 radicals can be consumed:

- 294 • Reaction R2 represents the radical consumption due to reaction with
 295 naphthalene
- 296 • Reaction R3 represents the consumption of nitrogen radicals by quench-
 297 ing with bulk gas molecules producing non-reactive radicals that do not
 298 react with any naphthalene molecule.

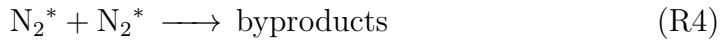
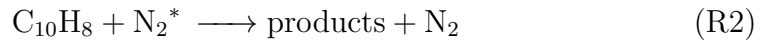
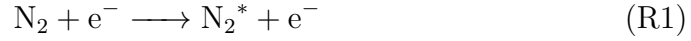


(a) Thermal cracking vs. plasma-enhanced thermal cracking of naphthalene

(b) Energy efficiency and plasma-enhanced thermal conversion vs. Temperature

Figure 6: Evolution of conversion and energy efficiency (EE) with temperature

- 299 • Reaction R4 represents the collisions between two radicals that lead
 300 to non-reactive radicals ,which do not react with any naphthalene
 301 molecule.



302 The main radical leading to tar cracking (N_2^*) is the metastable $\text{N}_2(\text{A}^3\Sigma)$,
 303 due to its higher reaction rate [46] and longer lifetime [69, 70]. In addi-
 304 tion to this metastable compound, other excited states can help to remove

305 naphthalene such $N_2(a'^1\Sigma_u^-)$, $N_2(a^1\Pi_g)$, $N_2(B^3\Pi_g)$ and $N_2(B^3\Sigma_u^-)$ [51]. Other
 306 reactions like excitation of naphthalene due to electron impact are not taken
 307 into account in this model due to the small electron cross sections of hydro-
 308 carbons together with the small concentration of naphthalene with respect
 309 to nitrogen [34].

310 The plasma naphthalene removal kinetics will depend on the way radicals
 311 are consumed. The ideal use of the radicals is the naphthalene removal given
 312 by the reaction R2, while reactions R3, R4 lead to inefficiencies.

313 By making a mass balance over the reactive species N_2^* , the radical ter-
 314 mination due to naphthalene removal and the radical termination due to
 315 collisions with bulk gas molecules lead to equations 6 and 7 respectively.

$$[C]_f - [C]_o = k_1 * SEI \quad (6)$$

$$\frac{[C]_f}{[C]_o} = exp\left(-\frac{SEI}{\beta}\right) \quad (7)$$

316 where $[C]_f$ and $[C]_o$ are expressed in mol/L, k_1 in mol/J and SEI and β
 317 in J/L.

318 The plot of the left side of the above equations with respect to SEI allows
 319 to determine which mechanism is followed during the removal process: if
 320 there is a linear trend between concentrations and SEI, plasma excited species
 321 are consumed by naphthalene decomposition while a logarithmic relationship
 322 between the ratio of final to initial concentrations and SEI indicates that
 323 plasma is consumed by collisions with the bulk gas. The aforementioned
 324 graphs are presented in figure 7, where none of the graphs shows a linear
 325 trend, however, comparing the two figures we can distinguish two different

326 regions.

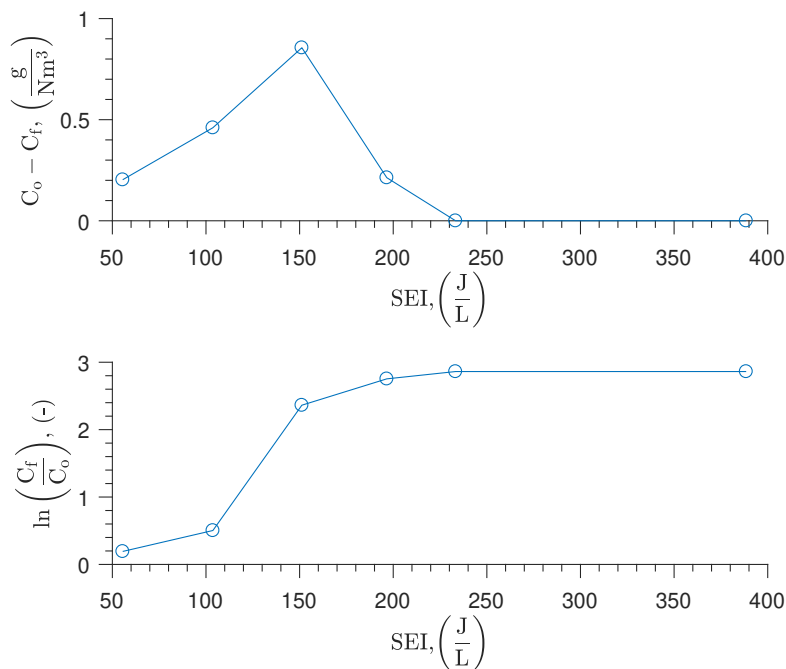


Figure 7: Plasma naphthalene removal with respect to SEI. Upper graph: No linear radical termination kinetics R2. Lower part: Linear radical termination kinetics R3

327 The first region, below and up to 800°C (corresponding to an SEI of 150
328 J/L) there is a linear proportionality between the concentrations and the SEI
329 in the upper graph of figure 7; this describes that in this region the naphtha-
330 lene removal is dominated by reactions with plasma reactive species. In the
331 second region, above 800°C, where there is a logarithmic proportionality be-
332 tween the ratio of concentrations and the SEI in the lower graph of 7; here the
333 plasma reactive species are consumed by collisions with bulk gas molecules,
334 indicating that the reduction of naphthalene concentration is dominated by
335 thermal cracking.

336 These results suggest that after a specific threshold, in this case 800°C,

337 thermal tar cracking modeling is sufficient to simulate tar removal. This
338 explains why the simulations of other researchers based on thermal crack-
339 ing only, are sufficient to describe the concentrations of tar after a thermal
340 plasma cleaning unit [27, 28, 30]. However further experiments need to be
341 performed in order to evaluate how the residence time can affect the thresh-
342 old where thermal cracking is dominant, since the study of Materazzi et al.
343 [28] evidences that at short residence times($<2s$), the effect of plasma excited
344 species can play a significant role for naphthalene and benzene removal.

345 **4. Conclusion**

346 Gasification of MSW is a promising technology for waste treatment and
347 energy valorization, but it is strongly limited by the presence of tar. MSW
348 gasification experiments showed that the most difficult tar compound to be
349 removed by thermal cracking is naphthalene. Naphthalene cracking was then
350 studied under a nanosecond-pulsed (ns-pulsed) plasma unit in a downstream
351 reactor, where total naphthalene removal was achieved at 800°C a tempera-
352 ture much lower than the one needed in thermal removal alone, which was
353 around 1000°C . A maximum energy efficiency was also reached at 800°C .

354 A global kinetic model shows that below 800°C , the main mechanism of
355 plasma excited species consumption is naphthalene cracking, while above this
356 temperature, the main consumption mechanism is through collisions with the
357 bulk gas. From these results, we can expect that with real tar, a temperature
358 well below 800°C is needed for complete tar removal using a plasma-aided
359 thermal plasma system since most of the compounds found in tar, with the
360 exception of PAHs heavier than tar, have a cracking temperature much lower

361 than the one of naphthalene. The optimal energy efficiency for real tar re-
362 moval is expected also to shift towards a lower temperature. An opposite
363 trend should be seen for benzene and heavy PAHs molecules like pyrene,
364 which need higher temperatures to be cracked [65, 71], expecting to have a
365 lower energy efficiency at a given temperature when compared to naphtha-
366 lene.

367 **Acknowledgement**

368 The research leading to these results has received funding from the Eu-
369 ropean Community’s Horizon 2020 Programme under Grant Agreement No.
370 721185 (MSCA-ETN NEW- MINE, <https://new-mine.eu/>). The main au-
371 thor also wants to thank Peter Colaerts and Dr. Radu Duca for their help-
372 ful discussions over the SPA/SPE analysis and Hans Van Eycken and Ivo
373 Lamberts for their helpful contributions to the mechanical fitting out of the
374 plasma reactor.

375 **References**

- 376 [1] J. Feroso, F. Rubiera, D. Chen, Sorption enhanced catalytic steam
377 gasification process: a direct route from lignocellulosic biomass to high
378 purity hydrogen, *Energy Environ. Sci.* 5 (2012) 6358–6367. URL:
379 <http://dx.doi.org/10.1039/C2EE02593K>. doi:10.1039/C2EE02593K.
- 380 [2] N. Kamińska-Pietrzak, A. Smoliński, Selected environmental
381 aspects of gasification and co-gasification of various types of
382 waste, *Journal of Sustainable Mining* 12 (2013) 6 – 13. URL:

- 383 <http://www.sciencedirect.com/science/article/pii/S230039601530063X>.
384 [doi:https://doi.org/10.7424/jsm130402](https://doi.org/10.7424/jsm130402).
- 385 [3] M. Hawrot-Paw, A. Koniuszy, M. Mikiciuk, M. Izwikow, T. Stawicki,
386 P. Sedlak, Analysis of ecotoxic influence of waste from the biomass gasifi-
387 cation process, *Environmental Science and Pollution Research* 24 (2017)
388 15022–15030. URL: <https://doi.org/10.1007/s11356-017-9011-8>.
389 [doi:10.1007/s11356-017-9011-8](https://doi.org/10.1007/s11356-017-9011-8).
- 390 [4] V. S. Sikarwar, M. Zhao, P. Clough, J. Yao, X. Zhong, M. Z. Memon,
391 N. Shah, E. J. Anthony, P. S. Fennell, An overview of advances in
392 biomass gasification, *Energy Environ. Sci.* 9 (2016) 2939–2977. URL:
393 <http://dx.doi.org/10.1039/C6EE00935B>. [doi:10.1039/C6EE00935B](https://doi.org/10.1039/C6EE00935B).
- 394 [5] Kim, T., Liu, G, Boaro, M, Lee, S.-I., Vohs, J, Gorte, R, Al-
395 Madhi, O, Dabbousi, B, A study of carbon formation and prevention in
396 hydrocarbon-fueled SOFC, *Journal of Power Sources* 155 (2006) 231–
397 238. URL: <http://dx.doi.org/10.1016/j.jpowsour.2005.05.001>.
398 [doi:10.1016/j.jpowsour.2005.05.001](https://doi.org/10.1016/j.jpowsour.2005.05.001).
- 399 [6] Lorente, E, Millan, M., Brandon, N., Use of gasification syngas in
400 SOFC: Impact of real tar on anode materials. , *International Jour-
401 nal of Hydrogen Energy* 37 (2012) 7271 – 7278. III Iberian Sympo-
402 sium on Hydrogen, Fuel Cells and Advanced Batteries, HYCELTEC-
403 2011. URL: <http://dx.doi.org/10.1016/j.ijhydene.2011.11.047>.
404 [doi:10.1016/j.ijhydene.2011.11.047](https://doi.org/10.1016/j.ijhydene.2011.11.047).
- 405 [7] Papurello, D., Lanzini, A., Leone, P, Santarelli, M., Vohs, J, Gorte, R,

- 406 Al-Madhi, O., Dabbousi, B., The effect of heavy tars (toluene and
407 naphthalene) on the electrochemical performance of an anode-supported
408 SOFC running on bio-syngas. , *Journal of Power Sources* 99 (2016) 747
409 – 753. URL: <http://dx.doi.org/10.1016/j.renene.2016.07.029>.
410 doi:10.1016/j.renene.2016.07.029.
- 411 [8] Subotić, V., Baldinelli, A., Barelli, L., Scharler, R., Pon-
412 gratz, G., Hochenauer, C., Anca-Couce, A., Applicability of
413 the SOFC technology for coupling with biomass-gasifier sys-
414 tems: Short- and long-term experimental study on SOFC per-
415 formance and degradation behaviour., *Applied Energy* 256 (2019).
416 URL: <http://dx.doi.org/10.1016/j.apenergy.2019.113904>.
417 doi:10.1016/j.apenergy.2019.113904.
- 418 [9] Bain, R. L., Dayton, D. C., Carpenter, D. L., Czernik, S. R.,
419 Feik, C. J., French, R. J., Magrini-Bair, K. A., Phillips, S. D., Eval-
420 uation of Catalyst Deactivation during Catalytic Steam Reforming of
421 Biomass-Derived Syngas., *Industrial & Engineering Chemistry Research*
422 44 (2005) 7945–7956. URL: <http://dx.doi.org/10.1021/ie050098w>.
423 doi:doi.org/10.1021/ie050098w.
- 424 [10] J. Zhou, H. Ma, F. Jin, H. Zhang, W. Ying, Mn and Mg dual
425 promoters modified Ni/ α -Al₂O₃ catalysts for high temperature syngas
426 methanation, *Fuel Processing Technology* 172 (2018) 225 – 232. URL:
427 <http://www.sciencedirect.com/science/article/pii/S0378382017311232>.
428 doi:<https://doi.org/10.1016/j.fuproc.2017.08.023>.
- 429 [11] P. Aravind, W. de Jong, Evaluation of high temperature gas cleaning

- 430 options for biomass gasification product gas for solid oxide fuel cells,
431 Progress in Energy and Combustion Science 38 (2012) 737 – 764. URL:
432 <http://www.sciencedirect.com/science/article/pii/S0360128512000214>.
433 doi:<https://doi.org/10.1016/j.pecs.2012.03.006>.
- 434 [12] S. Anis, Z. Zainal, Tar reduction in biomass producer gas via
435 mechanical, catalytic and thermal methods: A review, Renew-
436 able and Sustainable Energy Reviews 15 (2011) 2355 – 2377. URL:
437 <http://www.sciencedirect.com/science/article/pii/S1364032111000608>.
438 doi:<https://doi.org/10.1016/j.rser.2011.02.018>.
- 439 [13] X. Zeng, F. Wang, Y. Sun, J. Zhang, S. Tang, G. Xu, Characteristics
440 of tar abatement by thermal cracking and char catalytic reforming
441 in a fluidized bed two-stage reactor, Fuel 231 (2018) 18 – 25. URL:
442 <http://www.sciencedirect.com/science/article/pii/S0016236118308664>.
443 doi:<https://doi.org/10.1016/j.fuel.2018.05.043>.
- 444 [14] A. Warsita, K. Al-attab, Z. Zainal, Effect of water addition
445 in a microwave assisted thermal cracking of biomass tar mod-
446 els, Applied Thermal Engineering 113 (2017) 722 – 730. URL:
447 <http://www.sciencedirect.com/science/article/pii/S1359431116332045>.
448 doi:<https://doi.org/10.1016/j.applthermaleng.2016.11.076>.
- 449 [15] M. Zhai, X. Wang, Y. Zhang, P. Dong, G. Qi,
450 Y. Huang, Characteristics of rice husk tar secondary
451 thermal cracking, Energy 93 (2015) 1321 – 1327. URL:
452 <http://www.sciencedirect.com/science/article/pii/S0360544215013973>.
453 doi:<https://doi.org/10.1016/j.energy.2015.10.029>.

- 454 [16] C. P. Quitete, R. C. P. Bittencourt, M. M. Souza,
455 Coking resistance evaluation of tar removal catalysts,
456 Catalysis Communications 71 (2015) 79 – 83. URL:
457 <http://www.sciencedirect.com/science/article/pii/S1566736715300479>.
458 doi:<https://doi.org/10.1016/j.catcom.2015.08.013>.
- 459 [17] D. Meng, Y. Zhang, Z. Wang, X. Qu, J. Gao, T. Jiao,
460 P. Liang, Study on sulfur conversion characteristics in cat-
461 alytic cracking of coal tar in the presence of dolomite-
462 supported catalysts, Energy & Fuels 33 (2019) 5102–5109.
463 URL: <https://doi.org/10.1021/acs.energyfuels.9b00832>.
464 doi:10.1021/acs.energyfuels.9b00832.
- 465 [18] G. Guan, M. Kaewpanha, X. Hao, A. Abudula, Catalytic steam
466 reforming of biomass tar: Prospects and challenges, Renew-
467 able and Sustainable Energy Reviews 58 (2016) 450 – 461. URL:
468 <http://www.sciencedirect.com/science/article/pii/S1364032115016998>.
469 doi:<https://doi.org/10.1016/j.rser.2015.12.316>.
- 470 [19] S. Liu, Y. Wang, R. Wu, X. Zeng, S. Gao, G. Xu, Funda-
471 mentals of catalytic tar removal over in situ and ex situ chars in
472 two-stage gasification of coal, Energy & Fuels 28 (2014) 58–66.
473 URL: <https://doi.org/10.1021/ef4021153>. doi:10.1021/ef4021153.
474 arXiv:<https://doi.org/10.1021/ef4021153>.
- 475 [20] F. Di Gregorio, F. Parrillo, E. Salzano, F. Cammarota, U. Arena,
476 Removal of naphthalene by activated carbons from hot gas,
477 Chemical Engineering Journal 291 (2016) 244 – 253. URL:

- 478 <http://www.sciencedirect.com/science/article/pii/S1385894716300493>.
479 [doi:https://doi.org/10.1016/j.cej.2016.01.081](https://doi.org/10.1016/j.cej.2016.01.081).
- 480 [21] P. Lu, Q. Huang, Y. Chi, F. Wang, J. Yan, Catalytic cracking of tar de-
481 rived from the pyrolysis of municipal solid waste fractions over biochar,
482 Proceedings of the Combustion Institute 37 (2019) 2673 – 2680. URL:
483 <http://www.sciencedirect.com/science/article/pii/S1540748918302347>.
484 [doi:https://doi.org/10.1016/j.proci.2018.06.051](https://doi.org/10.1016/j.proci.2018.06.051).
- 485 [22] Y. Byun, W. Namkung, M. Cho, J. W. Chung, Y.-S. Kim,
486 J.-H. Lee, C.-R. Lee, S.-M. Hwang, Demonstration of ther-
487 mal plasma gasification/vitrification for municipal solid waste treat-
488 ment, Environmental Science & Technology 44 (2010) 6680–6684.
489 URL: <https://doi.org/10.1021/es101244u>. doi:10.1021/es101244u.
490 arXiv:<https://doi.org/10.1021/es101244u>, pMID: 20677789.
- 491 [23] Y. Byun, M. Cho, J. W. Chung, W. Namkung, H. D. Lee, S. D.
492 Jang, Y.-S. Kim, J.-H. Lee, C.-R. Lee, S.-M. Hwang, Hydro-
493 gen recovery from the thermal plasma gasification of solid waste,
494 Journal of Hazardous Materials 190 (2011) 317 – 323. URL:
495 <http://www.sciencedirect.com/science/article/pii/S0304389411003554>.
496 [doi:https://doi.org/10.1016/j.jhazmat.2011.03.052](https://doi.org/10.1016/j.jhazmat.2011.03.052).
- 497 [24] M. Hlina, M. Hrabovsky, T. Kavka, M. Konrad, Production
498 of high quality syngas from argon/water plasma gasification of
499 biomass and waste, Waste Management 34 (2014) 63 – 66. URL:
500 <http://www.sciencedirect.com/science/article/pii/S0956053X13004522>.
501 [doi:https://doi.org/10.1016/j.wasman.2013.09.018](https://doi.org/10.1016/j.wasman.2013.09.018).

- 502 [25] N. Agon, M. Hrabovsky, O. Chumak, M. Hlina, V. Kopecký, A. Masláni,
503 A. Bosmans, L. Helsen, S. Skoblja, G. V. Oost, J. Vierendeels, Plasma
504 gasification of refuse derived fuel in a single-stage system using differ-
505 ent gasifying agents, *Waste Management* 47 (2016) 246 – 255. URL:
506 <http://www.sciencedirect.com/science/article/pii/S0956053X15300313>.
507 doi:<https://doi.org/10.1016/j.wasman.2015.07.014>, refuse Derived
508 Fuel/Solid Recovered Fuel.
- 509 [26] A. Sanlisoy, M. Carpinlioglu, A review on plasma gasi-
510 fication for solid waste disposal, *International Jour-
511 nal of Hydrogen Energy* 42 (2017) 1361 – 1365. URL:
512 <http://www.sciencedirect.com/science/article/pii/S0360319916306735>.
513 doi:<https://doi.org/10.1016/j.ijhydene.2016.06.008>.
- 514 [27] M. Materazzi, P. Lettieri, L. Mazzei, R. Taylor, C. Chapman, Tar
515 evolution in a two stage fluid bed–plasma gasification process for waste
516 valorization, *Fuel Processing Technology* 128 (2014) 146 – 157. URL:
517 <http://www.sciencedirect.com/science/article/pii/S037838201400280X>.
518 doi:<https://doi.org/10.1016/j.fuproc.2014.06.028>.
- 519 [28] M. Materazzi, P. Lettieri, L. Mazzei, R. Taylor, C. Chap-
520 man, Reforming of tars and organic sulphur com-
521 pounds in a plasma-assisted process for waste gasification,
522 *Fuel Processing Technology* 137 (2015) 259 – 268. URL:
523 <http://www.sciencedirect.com/science/article/pii/S0378382015001174>.
524 doi:<https://doi.org/10.1016/j.fuproc.2015.03.007>.
- 525 [29] Y. Gómez-Rueda, L. Helsen, The role of plasma in syn-

- 526 gas tar cracking, *Biomass Conversion and Biorefinery*
527 (2019). URL: <https://doi.org/10.1007/s13399-019-00461-x>.
528 doi:10.1007/s13399-019-00461-x.
- 529 [30] F. Marias, R. Demarthon, A. Bloas, J. Robert-arnouil,
530 Modeling of tar thermal cracking in a plasma reactor,
531 *Fuel Processing Technology* 149 (2016) 139 – 152. URL:
532 <http://www.sciencedirect.com/science/article/pii/S0378382016301400>.
533 doi:<https://doi.org/10.1016/j.fuproc.2016.04.001>.
- 534 [31] S. Liu, D. Mei, L. Wang, X. Tu, Steam reforming of toluene
535 as biomass tar model compound in a gliding arc discharge reac-
536 tor, *Chemical Engineering Journal* 307 (2017) 793 – 802. URL:
537 <http://www.sciencedirect.com/science/article/pii/S1385894716310762>.
538 doi:<https://doi.org/10.1016/j.cej.2016.08.005>.
- 539 [32] T. Nunnally, A. Tsangaris, A. Rabinovich, G. Nirenberg, I. Cher-
540 nets, A. Fridman, Gliding arc plasma oxidative steam reforming of
541 a simulated syngas containing naphthalene and toluene, *Interna-
542 tional Journal of Hydrogen Energy* 39 (2014) 11976 – 11989. URL:
543 <http://www.sciencedirect.com/science/article/pii/S0360319914016073>.
544 doi:<https://doi.org/10.1016/j.ijhydene.2014.06.005>.
- 545 [33] H. Zhang, F. Zhu, X. Li, R. Xu, L. Li, J. Yan, X. Tu, Steam reforming
546 of toluene and naphthalene as tar surrogate in a gliding arc discharge
547 reactor, *Journal of Hazardous Materials* 369 (2019) 244 – 253. URL:
548 <http://www.sciencedirect.com/science/article/pii/S0304389419300925>.
549 doi:<https://doi.org/10.1016/j.jhazmat.2019.01.085>.

- 550 [34] Y. Wang, H. Yang, X. Tu, Plasma reforming of naphtha-
551 lene as a tar model compound of biomass gasification, *En-*
552 *ergy Conversion and Management* 187 (2019) 593 – 604. URL:
553 <http://www.sciencedirect.com/science/article/pii/S0196890419302663>.
554 doi:<https://doi.org/10.1016/j.enconman.2019.02.075>.
- 555 [35] X. Kong, H. Zhang, X. Li, R. Xu, I. Mubeen, L. Li, J. Yan, De-
556 struction of toluene, naphthalene and phenanthrene as model tar com-
557 pounds in a modified rotating gliding arc discharge reactor, *Cata-*
558 *lysts* 9 (2018) 19. URL: <http://dx.doi.org/10.3390/catal9010019>.
559 doi:10.3390/catal9010019.
- 560 [36] D. Mei, Y. Wang, S. Liu, M. Alliati, H. Yang, X. Tu,
561 Plasma reforming of biomass gasification tars using mixed
562 naphthalene and toluene as model compounds, *Energy*
563 *Conversion and Management* 195 (2019) 409 – 419. URL:
564 <http://www.sciencedirect.com/science/article/pii/S0196890419305412>.
565 doi:<https://doi.org/10.1016/j.enconman.2019.05.002>.
- 566 [37] D. Mei, S. Liu, Y. Wang, H. Yang, Z. Bo, X. Tu, Enhanced reforming
567 of mixed biomass tar model compounds using a hybrid gliding arc
568 plasma catalytic process, *Catalysis Today* 337 (2019) 225 – 233. URL:
569 <http://www.sciencedirect.com/science/article/pii/S0920586119302536>.
570 doi:<https://doi.org/10.1016/j.cattod.2019.05.046>, *frontiers in Plasma*
571 *Catalysis* (ISPCEM 2018).
- 572 [38] F. Saleem, K. Zhang, A. P. Harvey, Decomposition of benzene as
573 a tar analogue in CO₂ and H₂ carrier gases, using a non-thermal

- 574 plasma, *Chemical Engineering Journal* 360 (2019) 714 – 720. URL:
575 <http://www.sciencedirect.com/science/article/pii/S1385894718324288>.
576 doi:<https://doi.org/10.1016/j.cej.2018.11.195>.
- 577 [39] Z. Wu, J. Wang, J. Han, S. Yao, S. Xu, P. Martin, Naphtha-
578 lene decomposition by dielectric barrier discharges at atmospheric
579 pressure, *IEEE Transactions on Plasma Science* 45 (2017) 154–161.
580 doi:[10.1109/TPS.2016.2632154](https://doi.org/10.1109/TPS.2016.2632154).
- 581 [40] L. Liu, Q. Wang, S. Ahmad, X. Yang, M. Ji, Y. Sun, Steam reforming of
582 toluene as model biomass tar to H₂-rich syngas in a dbd plasma-catalytic
583 system, *Journal of the Energy Institute* 91 (2018) 927 – 939. URL:
584 <http://www.sciencedirect.com/science/article/pii/S1743967117305755>.
585 doi:<https://doi.org/10.1016/j.joei.2017.09.003>.
- 586 [41] S. Liu, D. Mei, M. Nahil, S. Gadkari, S. Gu, P. Williams,
587 X. Tu, Hybrid plasma-catalytic steam reforming of toluene
588 as a biomass tar model compound over Ni/Al₂O₃ catalysts,
589 *Fuel Processing Technology* 166 (2017) 269 – 275. URL:
590 <http://www.sciencedirect.com/science/article/pii/S0378382017304952>.
591 doi:<https://doi.org/10.1016/j.fuproc.2017.06.001>.
- 592 [42] L. Liu, Q. Wang, J. Song, S. Ahmad, X. Yang, Y. Sun,
593 Plasma-assisted catalytic reforming of toluene to hydrogen rich syn-
594 gas, *Catalysis Science & Technology* 7 (2017) 4216–4231. URL:
595 <http://dx.doi.org/10.1039/C7CY00970D>. doi:[10.1039/C7CY00970D](https://doi.org/10.1039/C7CY00970D).
- 596 [43] R. Cimerman, D. Račková, K. Hensel, Tars removal by non-thermal

- 597 plasma and plasma catalysis, *Journal of Physics D: Applied Physics* 51
598 (2018). doi:10.1088/1361-6463/aac762.
- 599 [44] L. Liu, Y. Liu, J. Song, S. Ahmad, J. Liang, Y. Sun, Plasma-enhanced
600 steam reforming of different model tar compounds over ni-based fu-
601 sion catalysts, *Journal of Hazardous Materials* 377 (2019) 24 – 33. URL:
602 <http://www.sciencedirect.com/science/article/pii/S0304389419305527>.
603 doi:<https://doi.org/10.1016/j.jhazmat.2019.05.019>.
- 604 [45] S. Nair, K. Yan, A. Pemen, G. Winands, F. van Gompel,
605 H. van Leuken, E. van Heesch, K. Ptasinski, A. Drinkenburg,
606 A high-temperature pulsed corona plasma system for fuel gas
607 cleaning, *Journal of Electrostatics* 61 (2004) 117 – 127. URL:
608 <http://www.sciencedirect.com/science/article/pii/S0304388604000397>.
609 doi:<https://doi.org/10.1016/j.elstat.2004.02.002>.
- 610 [46] V. A. Bityurin, E. A. Filimonova, G. V. Naidis, Simulation of
611 naphthalene conversion in biogas initiated by pulsed corona dis-
612 charges, *IEEE Transactions on Plasma Science* 37 (2009) 911–919.
613 doi:10.1109/TPS.2009.2019756.
- 614 [47] F. Saleem, K. Zhang, A. Harvey, Temperature dependence
615 of non-thermal plasma assisted hydrocracking of toluene to
616 lower hydrocarbons in a dielectric barrier discharge reactor,
617 *Chemical Engineering Journal* 356 (2019) 1062 – 1069. URL:
618 <http://www.sciencedirect.com/science/article/pii/S1385894718315171>.
619 doi:<https://doi.org/10.1016/j.cej.2018.08.050>.

- 620 [48] L. Devi, K. J. Ptasinski, F. J. Janssen, S. V. van Paasen, P. C. Bergman,
621 J. H. Kiel, Catalytic decomposition of biomass tars: use of dolomite
622 and untreated olivine, *Renewable Energy* 30 (2005) 565 – 587. URL:
623 <http://www.sciencedirect.com/science/article/pii/S0960148104002927>.
624 doi:<https://doi.org/10.1016/j.renene.2004.07.014>.
- 625 [49] L. P. L. M. Rabou, R. W. R. Zwart, B. J. Vreugdenhil, L. Bos, Tar in
626 biomass producer gas, the Energy Research Centre of the Netherlands
627 (ECN) experience: An enduring challenge, *Energy & Fuels* 23 (2009)
628 6189–6198. doi:10.1021/ef9007032.
- 629 [50] C. Brage, Q. Yu, G. Chen, K. Sjöström, Use of amino phase adsorbent
630 for biomass tar sampling and separation, *Fuel* 76 (1997) 137 – 142. URL:
631 <http://www.sciencedirect.com/science/article/pii/S0016236196001998>.
632 doi:[https://doi.org/10.1016/S0016-2361\(96\)00199-8](https://doi.org/10.1016/S0016-2361(96)00199-8).
- 633 [51] A. A. Abdelaziz, T. Seto, M. Abdel-Salam, Y. Otani, Influence
634 of nitrogen excited species on the destruction of naphthalene
635 in nitrogen and air using surface dielectric barrier discharge,
636 *Journal of Hazardous Materials* 246-247 (2013) 26 – 33. URL:
637 <http://www.sciencedirect.com/science/article/pii/S0304389412011703>.
638 doi:<https://doi.org/10.1016/j.jhazmat.2012.12.005>.
- 639 [52] M. Redolfi, N. Blin-Simiand, X. Duten, S. Pasquiers, K. Hassouni,
640 Naphthalene oxidation by different non-thermal electrical discharges at
641 atmospheric pressure, *Plasma Science and Technology* 21 (2019) 055503.
642 doi:10.1088/2058-6272/ab01c7.

- 643 [53] G. Ravenni, O. Elhami, J. Ahrenfeldt, U. Henriksen, Y. Neubauer,
644 Adsorption and decomposition of tar model compounds over the
645 surface of gasification char and active carbon within the tempera-
646 ture range 250–800°C, *Applied Energy* 241 (2019) 139 – 151. URL:
647 <http://www.sciencedirect.com/science/article/pii/S0306261919304313>.
648 doi:<https://doi.org/10.1016/j.apenergy.2019.03.032>.
- 649 [54] J. Zeng, J. Hu, Y. Qiu, S. Zhang, D. Zeng, R. Xiao,
650 Multi-function of oxygen carrier for in-situ tar removal
651 in chemical looping gasification: Naphthalene as a model
652 compound, *Applied Energy* 253 (2019) 113502. URL:
653 <http://www.sciencedirect.com/science/article/pii/S0306261919311766>.
654 doi:<https://doi.org/10.1016/j.apenergy.2019.113502>.
- 655 [55] W. Yu, S. Han, Z. Lei, K. Zhang, J. Yan, Z. Li, H. Shui, S. Kang,
656 Z. Wang, S. Ren, C. Pan, The reaction behavior of volatiles
657 generated from lignite pyrolysis, *Fuel* 244 (2019) 22 – 30. URL:
658 <http://www.sciencedirect.com/science/article/pii/S0016236119301851>.
659 doi:<https://doi.org/10.1016/j.fuel.2019.01.185>.
- 660 [56] Q. Zhou, Q. Liu, L. Shi, Y. Yan, J. Wu, C. Xiang, T. Wang, Z. Liu,
661 Effect of volatiles' reaction on composition of tars derived from pyrolysis
662 of a lignite and a bituminous coal, *Fuel* 242 (2019) 140 – 148. URL:
663 <http://www.sciencedirect.com/science/article/pii/S0016236119300067>.
664 doi:<https://doi.org/10.1016/j.fuel.2019.01.005>.
- 665 [57] M. Kuba, H. Hofbauer, Experimental parametric study on prod-
666 uct gas and tar composition in dual fluid bed gasification of

- 667 woody biomass, *Biomass and Bioenergy* 115 (2018) 35 – 44. URL:
668 <http://www.sciencedirect.com/science/article/pii/S0961953418300965>.
669 doi:<https://doi.org/10.1016/j.biombioe.2018.04.007>.
- 670 [58] T.-Y. Mun, B.-S. Kang, J.-S. Kim, Production of a pro-
671 ducer gas with high heating values and less tar from dried
672 sewage sludge through air gasification using a two-stage gasifier
673 and activated carbon, *Energy & Fuels* 23 (2009) 3268–3276.
674 URL: <https://doi.org/10.1021/ef900028n>. doi:10.1021/ef900028n.
675 arXiv:<https://doi.org/10.1021/ef900028n>.
- 676 [59] Q. Jin, X. Wang, S. Li, H. Mikulčić, T. Bešenić, S. Deng, M. Vujanović,
677 H. Tan, B. M. Kumfer, Synergistic effects during co-pyrolysis of
678 biomass and plastic: Gas, tar, soot, char products and thermogravimet-
679 ric study, *Journal of the Energy Institute* 92 (2019) 108 – 117. URL:
680 <http://www.sciencedirect.com/science/article/pii/S1743967117307122>.
681 doi:<https://doi.org/10.1016/j.joei.2017.11.001>.
- 682 [60] A. Veksha, A. Giannis, G. Yuan, J. Tng, W. P. Chan, V. W.-
683 C. Chang, G. Lisak, T.-T. Lim, Distribution and modeling of
684 tar compounds produced during downdraft gasification of municipi-
685 pal solid waste, *Renewable Energy* 136 (2019) 1294 – 1303. URL:
686 <http://www.sciencedirect.com/science/article/pii/S0960148118311819>.
687 doi:<https://doi.org/10.1016/j.renene.2018.09.104>.
- 688 [61] M. Irfan, A. Li, L. Zhang, M. Wang, C. Chen, S. Khushk, Pro-
689 duction of hydrogen enriched syngas from municipal solid waste

- 690 gasification with waste marble powder as a catalyst, *International Journal of Hydrogen Energy* 44 (2019) 8051 – 8061. URL:
691 <http://www.sciencedirect.com/science/article/pii/S0360319919306329>.
692 doi:<https://doi.org/10.1016/j.ijhydene.2019.02.048>.
- 694 [62] C. Block, A. Ephraïm, E. Weiss-Hortala, D. P. Minh, A. Nzihou,
695 C. Vandecasteele, Co-pyrogasification of plastics and biomass, a re-
696 view, *Waste and Biomass Valorization* 10 (2019) 483–509. URL:
697 <https://doi.org/10.1007/s12649-018-0219-8>. doi:10.1007/s12649-
698 018-0219-8.
- 699 [63] G. Lopez, A. Erkiaga, M. Amutio, J. Bilbao, M. Olazar, Effect
700 of polyethylene co-feeding in the steam gasification of biomass
701 in a conical spouted bed reactor, *Fuel* 153 (2015) 393 – 401. URL:
702 <http://www.sciencedirect.com/science/article/pii/S0016236115002872>.
703 doi:<https://doi.org/10.1016/j.fuel.2015.03.006>.
- 704 [64] M. Cortazar, J. Alvarez, G. Lopez, M. Amutio, L. Santamaria, J. Bil-
705 bao, M. Olazar, Role of temperature on gasification performance and
706 tar composition in a fountain enhanced conical spouted bed reactor,
707 *Energy Conversion and Management* 171 (2018) 1589 – 1597. URL:
708 <http://www.sciencedirect.com/science/article/pii/S0196890418306812>.
709 doi:<https://doi.org/10.1016/j.enconman.2018.06.071>.
- 710 [65] A. Jess, Mechanisms and kinetics of thermal reactions of aromatic hydro-
711 carbons from pyrolysis of solid fuels, *Fuel* 75 (1996) 1441 – 1448. URL:
712 <http://www.sciencedirect.com/science/article/pii/0016236196001366>.
713 doi:[https://doi.org/10.1016/0016-2361\(96\)00136-6](https://doi.org/10.1016/0016-2361(96)00136-6).

- 714 [66] E. A. Filimonova, Y. ho Kim, S. H. Hong, Y.-H. Song, Multiparametric
715 investigation on NOxremoval from simulated diesel exhaust with hy-
716 drocarbons by pulsed corona discharge, *Journal of Physics D: Applied*
717 *Physics* 35 (2002) 2795–2807. doi:10.1088/0022-3727/35/21/316.
- 718 [67] Y. Gómez-Rueda, I. Nuran Zaini, W. Yang, L. Helsen, Landfill solid
719 waste-based syngas purification by a hybrid pulsed corona plasma
720 unit, 27th European Biomass Conference and Exhibition, 27-30 May
721 2019, Lisbon, Portugal (2019) 520 – 522. doi:10.5071/27thEUBCE2019-
722 2BO.6.2.
- 723 [68] K. Yan, E. J. M. van Heesch, A. J. M. Pemen, P. A. H. J. Hui-
724 jbrechts, From chemical kinetics to streamer corona reactor and volt-
725 age pulse generator, *Plasma Chemistry and Plasma Processing* 21
726 (2001) 107–137. URL: <https://doi.org/10.1023/A:1007045529652>.
727 doi:10.1023/A:1007045529652.
- 728 [69] A. M. Wróbel, I. Błaszczuk, A. Walkiewicz-Pietrzykowska, A. Tracz,
729 J. E. Klemberg-Sapieha, T. Aoki, Y. Hatanaka, Remote hydrogen-
730 nitrogen plasma chemical vapor deposition from a tetramethyldisi-
731 lazane source. part 1. mechanism of the process, structure and sur-
732 face morphology of deposited amorphous hydrogenated silicon carboni-
733 tride films, *Journal of Materials Chemistry* 13 (2003) 731–737. URL:
734 <http://dx.doi.org/10.1039/B211415C>. doi:10.1039/B211415C.
- 735 [70] Y. Choi, J. Kim, Y. Hwang, One-dimensional dis-
736 charge simulation of nitrogen dbd atmospheric pressure
737 plasma, *Thin Solid Films* 506-507 (2006) 389 – 395. URL:

738 <http://www.sciencedirect.com/science/article/pii/S004060900501299X>.
739 doi:<https://doi.org/10.1016/j.tsf.2005.08.103>, 7th Asia Pacific Con-
740 ference on Plasma Science and Technology (APCPST) and 17th
741 Symposium on Plasma Science for Materials (SPSM).

742 [71] R. Pujro, M. Falco, U. Sedran, Catalytic cracking of heavy
743 aromatics and polycyclic aromatic hydrocarbons over fluidized cat-
744 alytic cracking catalysts, *Energy & Fuels* 29 (2015) 1543–1549.
745 URL: <https://doi.org/10.1021/ef502707w>. doi:10.1021/ef502707w.
746 arXiv:<https://doi.org/10.1021/ef502707w>.